

636192



~~0~~
0

DDC
AUG 1 1966
PR

UTAH

CLEARINGHOUSE FOR FEDERAL SCIENTIFIC AND TECHNICAL INFORMATION			
Hardcopy	Microfilm		
\$ 2.00	\$.50	33 pp	7/2
ARCHIVE COPY			

NC.

36131

SPONSORED BY

Advanced Research Projects Agency
U. S. Army Natick Laboratories
Natick, Massachusetts
ARPA Order No. 267 Amendment No. 4

THEORETICAL AND EXPERIMENTAL STUDY
OF
LOW-VELOCITY PENETRATION PHENOMENA

SEMIANNUAL REPORT

December 1965

Contract DA-19-129-AMC-150(X)

Utah Research & Development Co., Inc
1820 South Industrial Road
Salt Lake City, Utah

362 750

Phone: 801/486-1301

34131

CONTRACT INFORMATION

Contract No. DA 19-129-AMC-150(X)

Order No. 267, Amend. No. 4 - 97X0400.1301 360-0267
P3860-200-S19-129

Program Code No. 3860

Contractor: Utah Research & Development Co., Inc.

Date of Contract: 25 June 1963

Amount of Contract: \$97,392.96 (Includes fixed fee of
\$7,214.29)

Supplemental Agreement: 22 May 1964

Amount of Supplemental Agreement: \$197,117.00
(Includes fixed fee of \$14,601.00)

Contract Expiration Date: 1 May 1966 (Supplemental Agreement
No. 1, Modification No. 2)

Project Scientist: Dr. Emerson T. Cannon

Work Title: Theoretical and Experimental Study of Low
Velocity Penetration Phenomena

TABLE OF CONTENTS

	Page
CONTRACT INFORMATION	i
ABSTRACT	iii
1. INTRODUCTION	1
2. THEORETICAL STUDIES	2
2.1 Predictor/Corrector Routines	4
2.2 Viscosity and Strength	9
2.3 Changes in the Model	11
3. EXPERIMENTAL WORK	17
3.1 Disc-Crushing Experiment	17
3.2 Dynamic Strength Measurements	17
3.2.1 Experimental System for Dynamic Measurements	18
3.2.2 Data from Dynamic Measurements	22
4. CONCLUSIONS	27
5. FUTURE WORK	28

ABSTRACT

Progress is reported on the development of a computer code for describing the flow field during impact of solid on solid. A one-dimensional material model is used consisting of isolated mass points connected by springs with highly non-linear spring constants and viscous damping. The spring constant is derived from shock Hugoniot equation-of-state work and the viscosity comes from measurements of the energy involved in crushing discs of the material used. So far, aluminum has been the only material tested in the computer program. The results of varying the predictor/corrector scheme used to stabilize the solution and the results of varying viscosity are presented. It is shown that the solution gives the correct pressure jump across a shock front and gives correct wave velocities. Some oscillations and propagation of error are present. Methods of improving this are discussed.

A rod-to-rod impact experiment is described for measuring the maximum pressure gradient which a material can sustain under dynamic impact conditions. The method is suitable for measuring material-strength properties for brittle materials which are not suited to the disc-crushing experiments previously used. Results are presented for nylon, polypropylene, plexiglass, Benelex, and glass. The plastics show a maximum pressure gradient, then a leveling off as impact velocity is increased. Glass increases continually up to the maximum velocities tested. Further work to increase the pressure used in the tests and to investigate geometric effects is outlined.

1. INTRODUCTION

The purpose of research done under this contract is to develop a theoretical and experimental basis for predicting the behavior of materials under impact. Materials of interest range from simple homogeneous materials such as metals or ceramics to complex structures made up of a variety of materials. Impact velocities of interest range from a few hundred to a few thousand feet per second. Our approach to the solution of this problem has been to develop a computer program to solve the transient flow field for the impact of one solid body on another. At this time a simplified program has been developed for the case of one-dimensional impact. More versatile codes are being studied and the work is progressing on developing the mathematical model and the computer program. All of the computations made so far have used the one-dimensional code so that the results can be checked by analytical calculations. This theoretical work will be discussed in this report. It has consisted primarily of an investigation of computer methods, particularly the investigation of predictor/corrector routines to stabilize the calculations and give a reasonable picture based on the mathematical model used. The effects of varying material properties in the computer code have been investigated. Viscosity has been varied over a range of values with a center value chosen from experimental results. The results of this investigation will be reported. A brief discussion will be given of the ways of improving this model and our projected future work in this area.

During this report period experimental work has consisted primarily of developing techniques for making dynamic-strength measurements of brittle materials. This was done by impacting rods of the material shot from an air gun against a similar stationary rod and measuring the acceleration of the face of the stationary rod. From this, an effective strength can be calculated. The results of this work are preliminary and as yet none of these materials have been used in the computer program. The data are in a form suitable for the present computer program and further exploratory work is contemplated in which the experimental results are used in the program and conditions varied to obtain agreement between the experiment and theory. In addition to this work, some further work was done on the disc-crushing experiment reported in the last semi-annual report. In particular, experiments were made to measure the friction involved between the disc and the anvil.

2. THEORETICAL STUDIES

A one-dimensional impact code has been devised based on the material model shown in Figure 1. In this model the mass is made up of discrete particles separated initially by a uniform distance. As the two semi-infinite sheets collide, particles are displaced and the forces acting on them are computed by the compression and the internal energy of the material. In effect, the model is that of discrete masses connected by springs which have peculiar non-linear spring constants and non-linear viscosity factors. The discrete-variable equations are derived from the usual continuous flow equations as shown here.

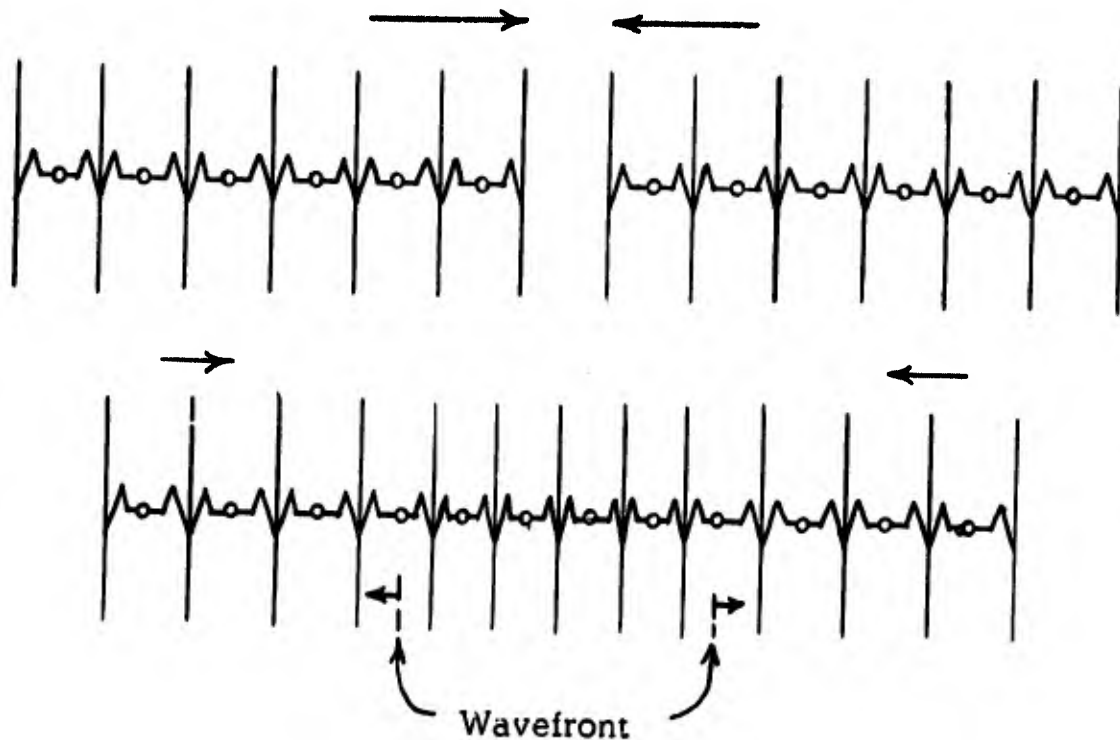


Figure 1. Discrete-particle model for one-dimensional impact. The material is shown before and after impact.

Momentum

$$\rho \frac{Dv}{Dt} = - \frac{\partial p}{\partial x} - \frac{\partial \tau}{\partial x}$$

$$\rho \frac{\Delta v}{\Delta t} = - \frac{(p|_{x+\Delta x} - p|_x)}{\Delta x} - \frac{(\tau|_{x+\Delta x} - \tau|_x)}{\Delta x}$$

Energy

$$\rho \frac{DU}{Dt} = - p \frac{\partial v}{\partial x} - \tau \frac{\partial v}{\partial x}$$

$$\rho \frac{\Delta U}{\Delta t} = - \frac{p(v|_{x+\Delta x} - v|_x)}{\Delta x} - \frac{\tau(v|_{x+\Delta x} - v|_x)}{\Delta x}$$

Hugoniot Equation of State

$$p = \frac{2}{M} \rho U^{1-k}$$

Viscosity

$$\tau = \mu_0 \frac{\partial v}{\partial x} \pm \tau_0$$

$$\tau = \mu_0 \frac{(v|_{x+\Delta x} - v|_x)}{\Delta x} \pm \tau_0$$

$\frac{D}{Dt}$ is the substantial derivative or derivative following the motion, ρ is density, v is velocity, p is pressure, x is distance, τ is the stress tensor (one term here), U is internal energy per unit mass, and M , k , μ_0 , and τ_0 are constants.

This model was chosen as being the most simple possible which would still allow a variation of important parameters to investigate their effects on the outcome.

2.1 Predictor/Corrector Routines

The procedure for solving the model is to use a predictor/corrector scheme. From the initial forces on each mass particle and the initial velocities, a new position is predicted as a first trial by using Newton's Laws as expressed in the momentum equation. The corrector is then called into play and used to improve the first guess and give a second guess. This is done by computing the forces on the particle at the time of the first new position and then calculating a corrected position by computing where the particle would have been if the force had varied linearly from the initial force to the final force. This corrected position is then the second new position. This process is repeated by computing the force as a result of the second position and predicting where a third position would have been if the force had varied linearly between the initial force and the force at the second position. This process results in fair predictions. In the first runs, the correction was made on each point in sequence; that is, one correction was made for all points in order from one end of the mesh to the other, then a second correction made for all points and so on. Better methods of doing this have been devised and are being programmed now. The first runs showed that the predictor rapidly propagates small errors throughout the entire mesh and that this error causes oscillation in the system. The results obtained by varying the number of corrections made are shown for a few computations in Figures 2, 3 and 4. These illustrate the problem and the care necessary in choosing the proper corrector and testing its performance. Figure 5 shows the displacement of several of the particles if the corrector is allowed to run on for long periods of time. It is seen how small amplitude oscillations develop and propagate. This particule corrector can be improved by limiting the propagation of error by limiting the distance through which the corrector can operate. This has been done as illustrated by merely limiting the number of times which the corrector can repeat. It can be done in another way by correcting each mass point individually as many times as desired, then going to the next mass point, correcting it, and using the corrected value of the first mass point and the second interacting with each other only once after they have been individually corrected. Various schemes such as this are being considered and the programs developed.

The actual force laws used in the corrector are a crude approximation and can be varied. Doing this is like performing an experiment and changing the variables: a variable is changed and a test is made; the variable is changed again, and another test is made. Once a basic program is developed, this can be done rapidly and inexpensively.

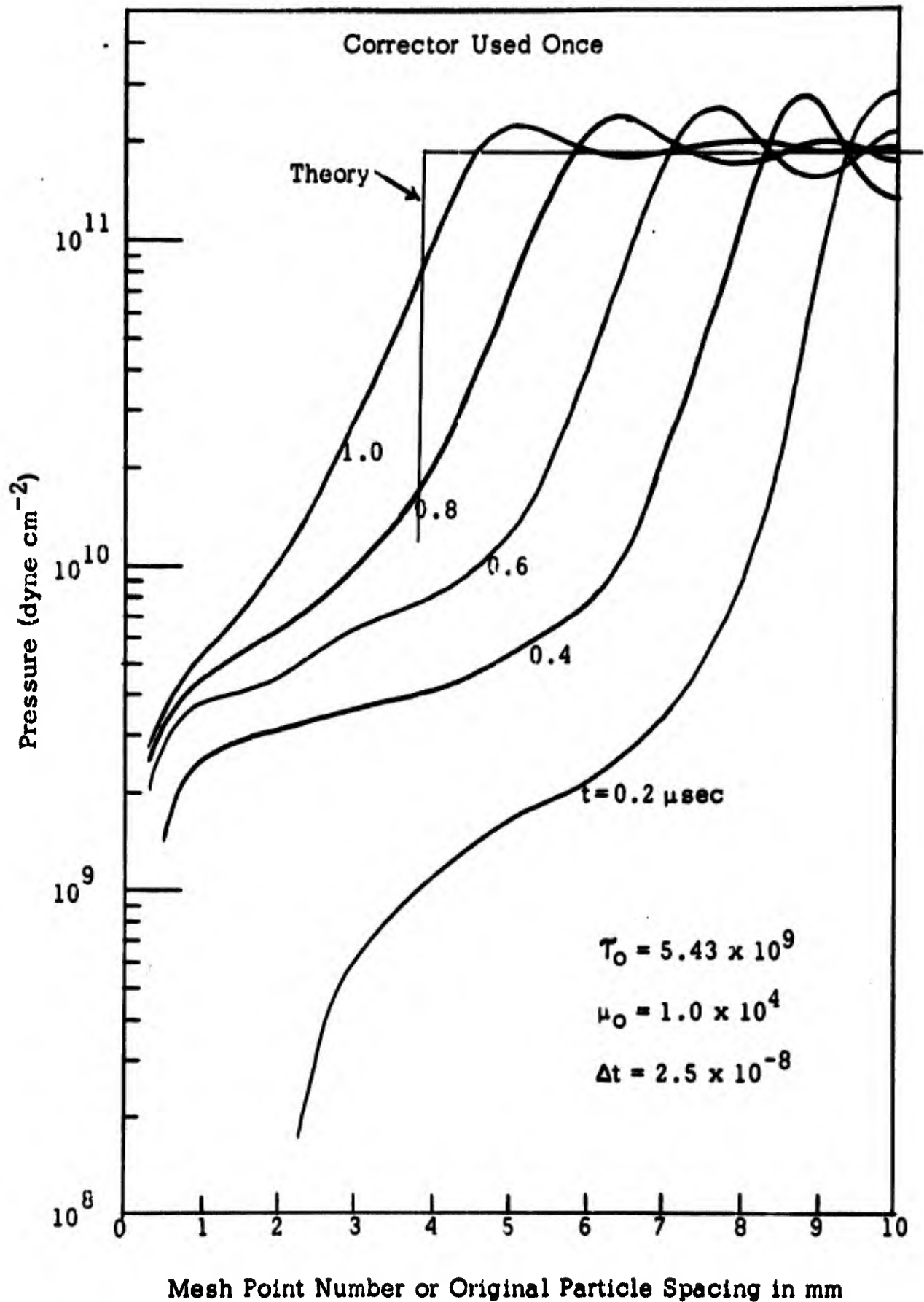


Figure 2. Pressure wave in one-dimensional impact in aluminum. Impact occurs at right hand side at $t = 0$, and wave progresses to the left. Compare Figures 2, 3 and 4 to see effects of changing the number of times the corrector is used. Curve marked "Theory" is from analytical calculations at $t = 1.0 \mu\text{sec}$.

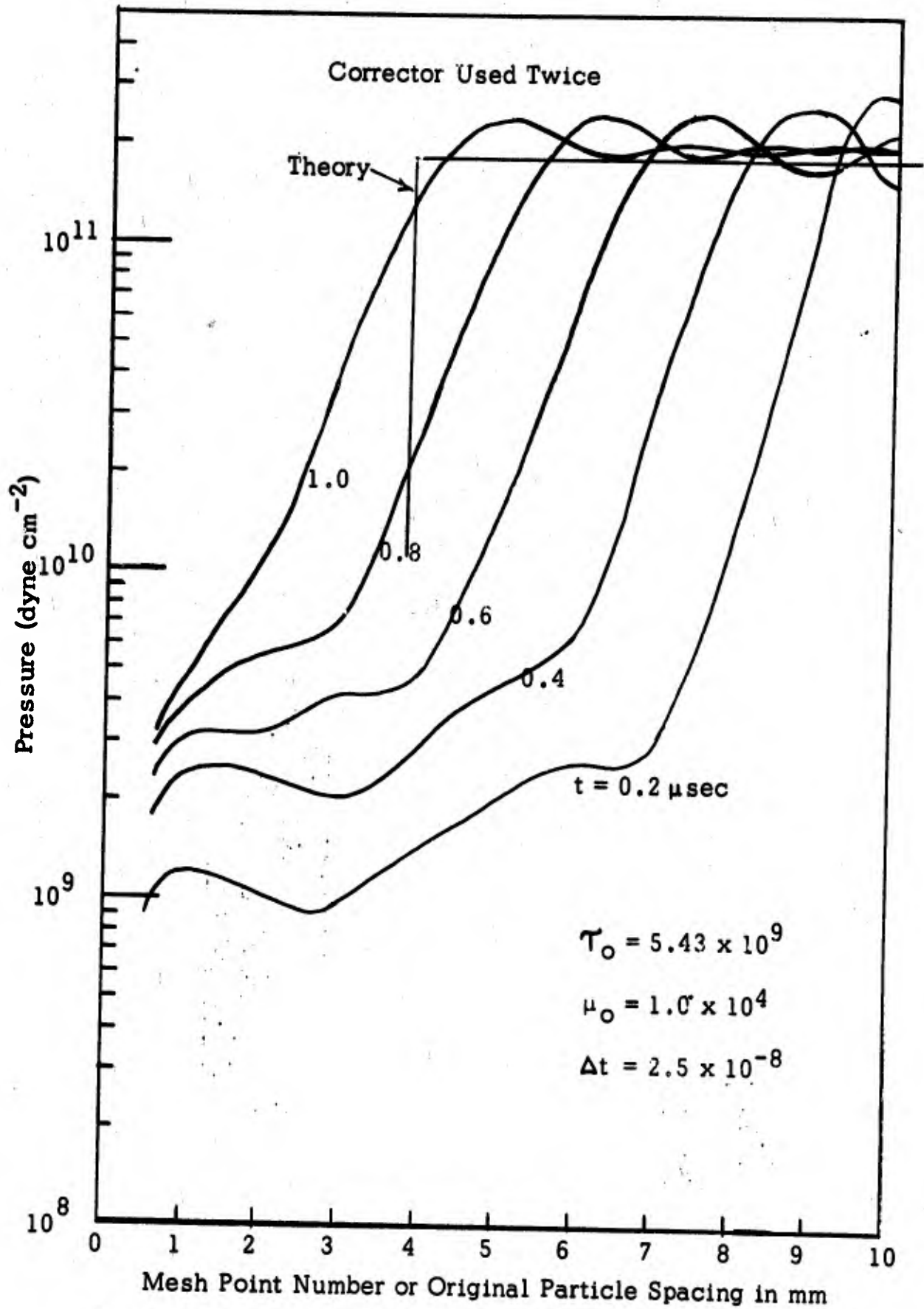


Figure 3. Pressure wave in one-dimensional impact in aluminum. Impact occurs at right hand side at $t = 0$, and wave progresses to the left. Compare Figures 2, 3 and 4 to see effects of changing the number of times the corrector is used. Curve marked "Theory" is from analytical calculations at $t = 1.0 \mu\text{sec}$.

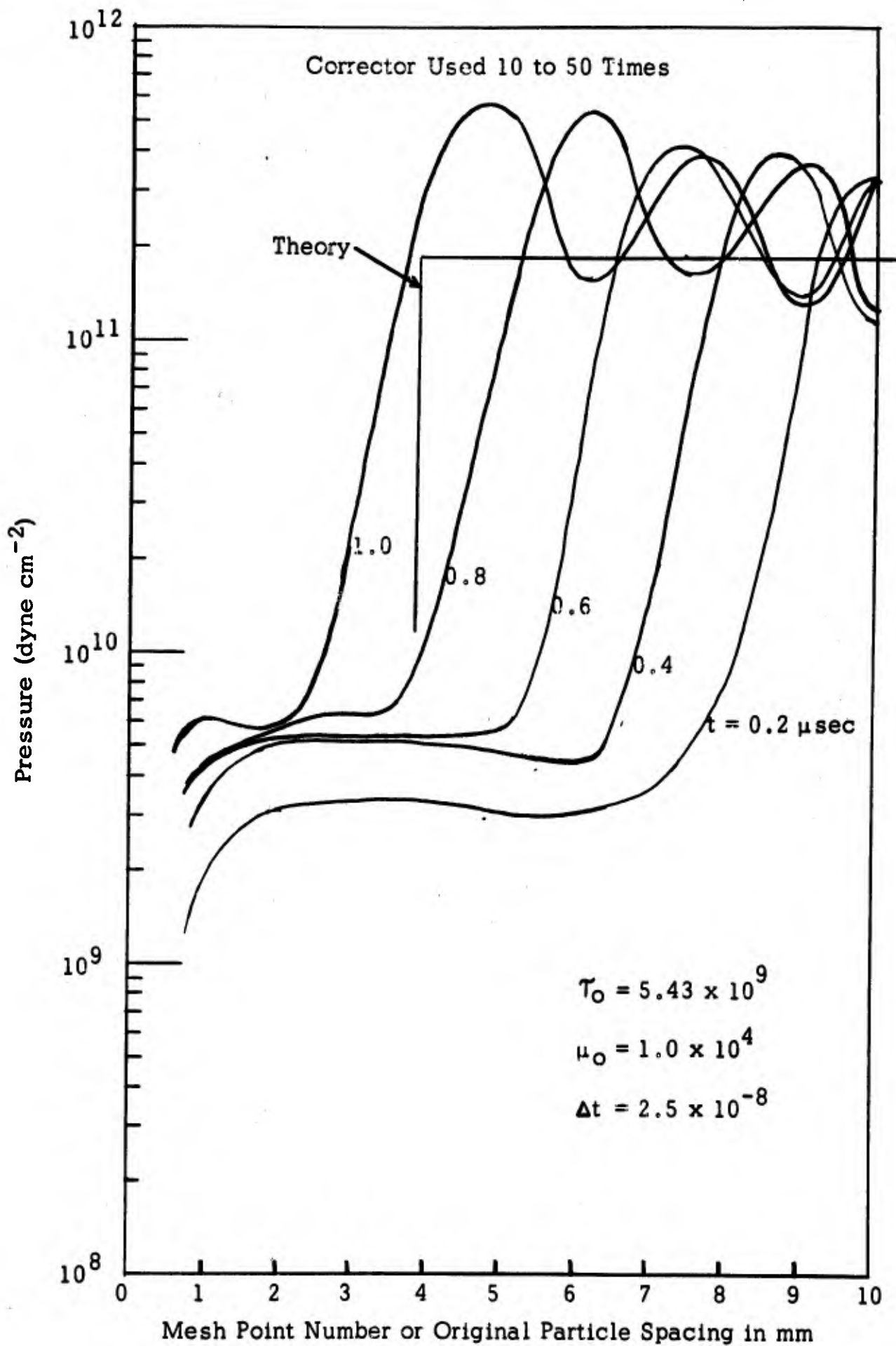


Figure 4. Pressure wave in one-dimensional impact in aluminum. Impact occurs at right hand side at $t = 0$, and wave progresses to the left. Compare Figures 2, 3 and 4 to see effects of changing the number of times the corrector is used. Curve marked "Theory" is from analytical calculations at $t = 1.0 \mu\text{sec}$.

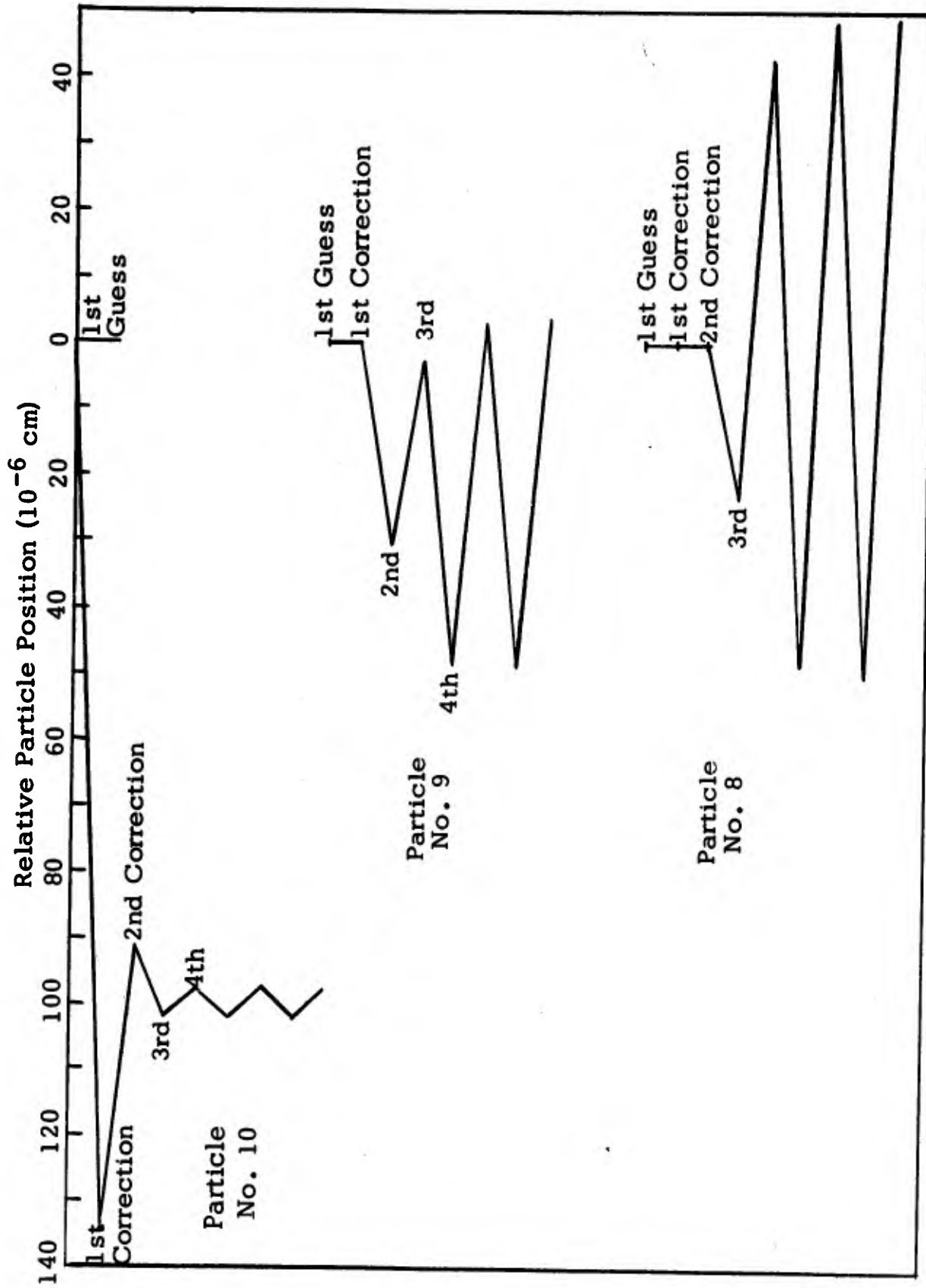


Figure 5. Plot of particle position relative to the first guess position for the first time increment after impact. Particle 10 collides with particle 11 at this time. Particles 1 to 7 behave similarly to 8 with a build up of small oscillations.

2.2 Viscosity and Strength

The initial computer runs were made without using viscosity. The Los Alamos equation of state was used to determine pressures, and it was found that the equation along the Hugoniot could be expressed in the following form:

$$\frac{\rho - \rho_0}{\rho_0} = MU^k \quad \text{or} \quad U = \left(\frac{\rho - \rho_0}{M\rho_0} \right)^{1/k}$$

Using this in the previously given equation of state gives

$$p = \frac{2}{M} \rho \left(\frac{\rho - \rho_0}{M\rho_0} \right)^{\frac{1-k}{k}}$$

The pressure is related only to density along the Hugoniot. This is a general form of equation that can be used for all metals reported by Los Alamos. The two constants are changed slightly for different metals. Since at the impact velocities used in this program the material departs only very slightly from the Hugoniot, this expression is adequate for both compression and expansion. This model fails to predict energies after expansion correctly or other expansion effects, but it was intended to be used only in compression during the advance of the first shock wave, so was adequate for first tests. Results of a run are shown in Figure 6. It is interesting to note that the correct shock wave pressure is predicted on the average, and the shock-wave velocity is about correct. The velocity could be varied by varying the way pressure was averaged from one cell to the next. In all the cases tried, it was close to the experimental value. It is somewhat surprising that these values were so close to the true values considering the large oscillations observed and the crude mathematical model used.

In an attempt to obtain a more correct model of the process, viscosity was introduced into the program. In this case pressure was not computed from the density, but was computed from the energy equation. Here the internal energy is a result of the compression and the viscous dissipation: the viscous dissipation adding continually to the energy while the compression energy is reversible. Since no true equation of state is available for these various energy states it was assumed that the pressure-volume-energy relationship paralleled that found along the Hugoniot and was displaced merely by the internal-energy equation. With this energy equation, the effects of expansion can be more correctly predicted and the residual energy after shock heating is determined. Residual expansion and heating of the material have not yet been definitely tested. This remains a work for the

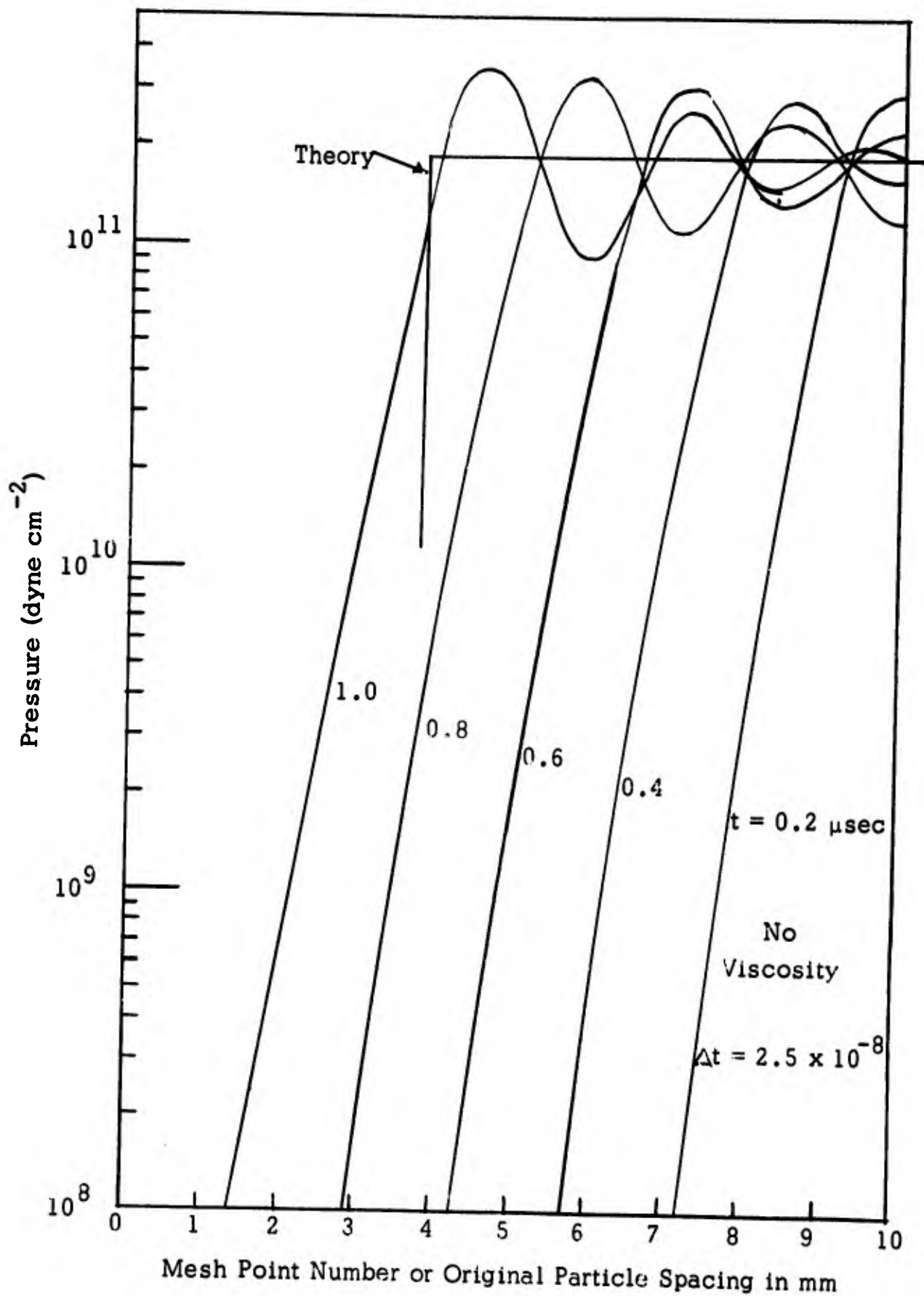


Figure 6. Pressure wave in one-dimensional impact in aluminum. Impact occurs at right hand side at $t = 0$, and wave progresses to the left. Results from computer program without viscosity. Corrector used three times; compare with Figure 3.

future and check on the over-all results. This viscosity used in this work was obtained from the disc-crushing experiment reported in the previous semi-annual report, and reproduced here for aluminum in Figure 7.

"Strength of the materials" can be adequately represented by a Bingham model. The strength term, τ_0 , is given by the initial slope of the line in Figure 7, and the viscous effect μ_0 , is given by the curvature; μ_0 is also related to the displacement of the static curve and the dynamic curve. From the data, the one-dimensional viscous strength term was given as follows:

$$\tau = \mu_0 \frac{\partial v}{\partial x} \pm \tau_0$$

$$\tau = (1.0 \times 10^4) \frac{\partial v}{\partial x} \pm 5.4 \times 10^9 \quad (\text{cgs units})$$

The program was run using the viscous force equation and the viscous energy equation and the above parameters. The corrector was varied and the viscosity was varied. Results of varying viscosity are shown in Figures 8, 9 and 10 for one particular corrector. It is seen that the use of the viscous equation dampens the oscillations, spreads the wave front out and in general gives values approximately correct as far as pressure jump and wave velocity are concerned.

2.3 Changes in the Model

Work has begun on changing the material model used and the computer scheme. This has not progressed far enough to report here in detail. One step in this direction is to change the scale of the experiment. By reducing the size of the time increment, the mass distribution becomes effectively much more uniform and approaches a distributed value rather than a system of discrete large masses. The results of one calculation are shown in Figure 11. This figure is best compared with Figure 9. A combination system using Lagrangian and Eulerian coordinates is being explored. This is a modified PIC code. In the PIC code, each individual mass particle of the material is moved according to the laws of motion, then the pressure and density gradients are computed from the number of particles present in each cell and their energy. In the modified code which we are considering, the cell boundaries change. Particles do not change cells but their motion determines the new cell boundary. The stress-strain relationships are more easily considered over the cells using the cell boundaries than using the particle positions. Whether this can be successfully implemented remains to be seen.

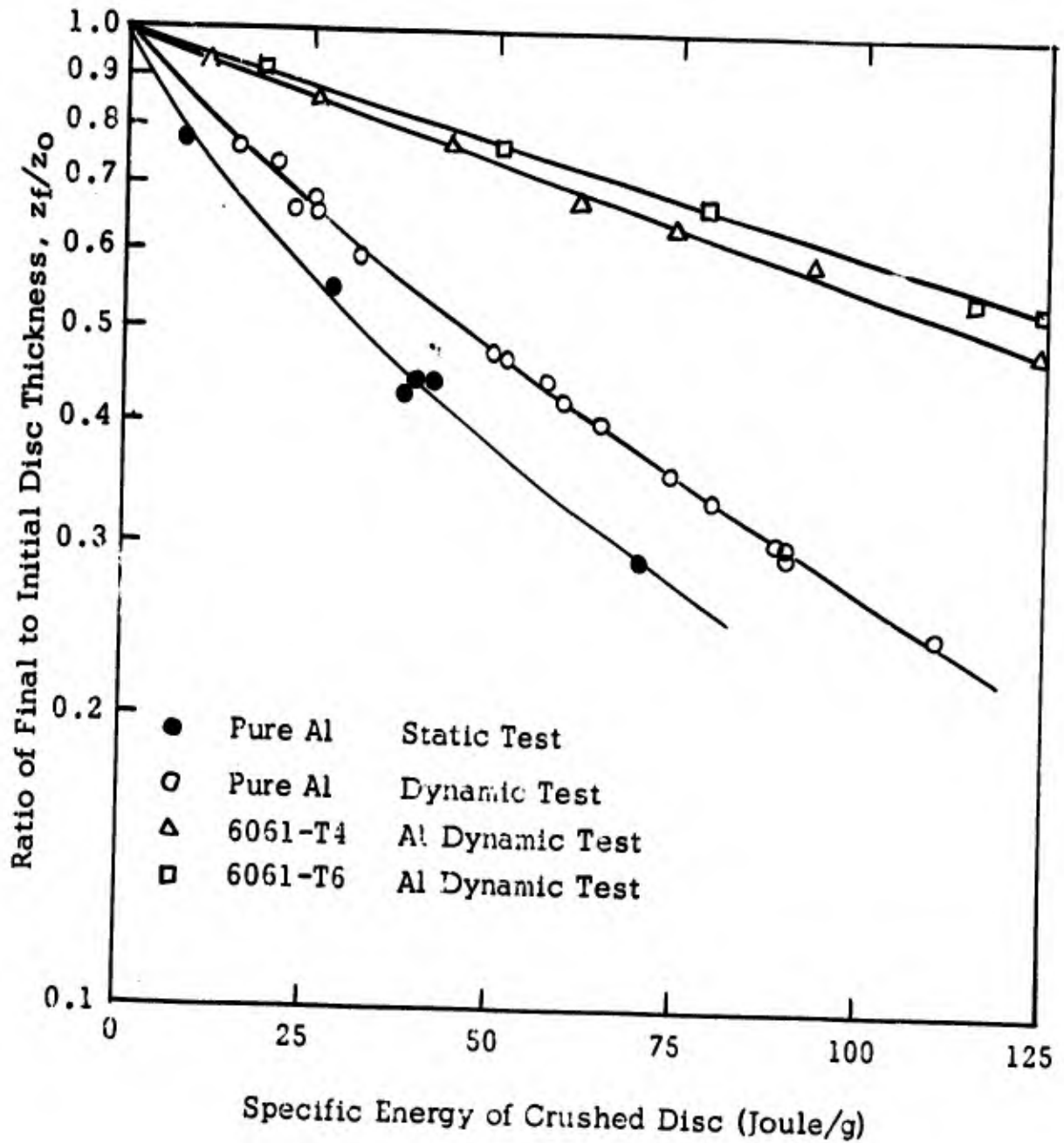


Figure 7. Energy required to crush aluminum discs. Constants τ_0 and μ_0 determined from the equations:

$$\rho U = \tau \ln(z_0/z_f)$$

$$\tau = \mu_0(\partial v/\partial x) + \tau_0$$

τ_0 determined from the initial slope of the curves. $\tau_0 = 5.43 \times 10^9$ from 6061 Al and 2.1×10^9 from pure Al.

μ_0 determined from difference between static and dynamic data for pure Al. $\partial v/\partial x = 3 \times 10^4$ from impact velocity and thickness of disc.

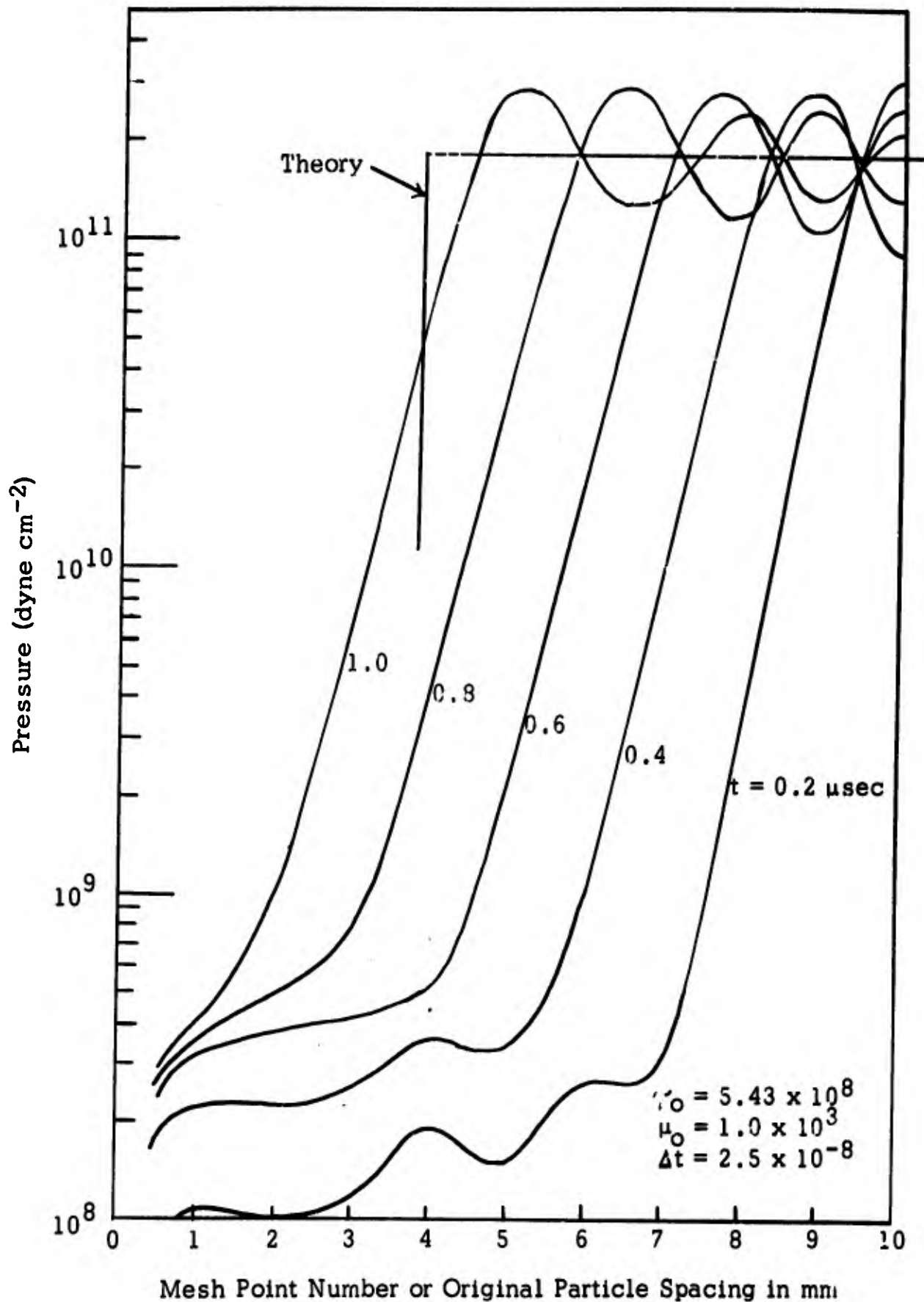


Figure 8. Pressure wave in one-dimensional impact in aluminum. Figures 8, 9 and 10 show the effects of varying viscosity. Corrector used twice in all cases. Curve marked "Theory" is from analytical calculations at $t = 1.0 \mu\text{sec}$.

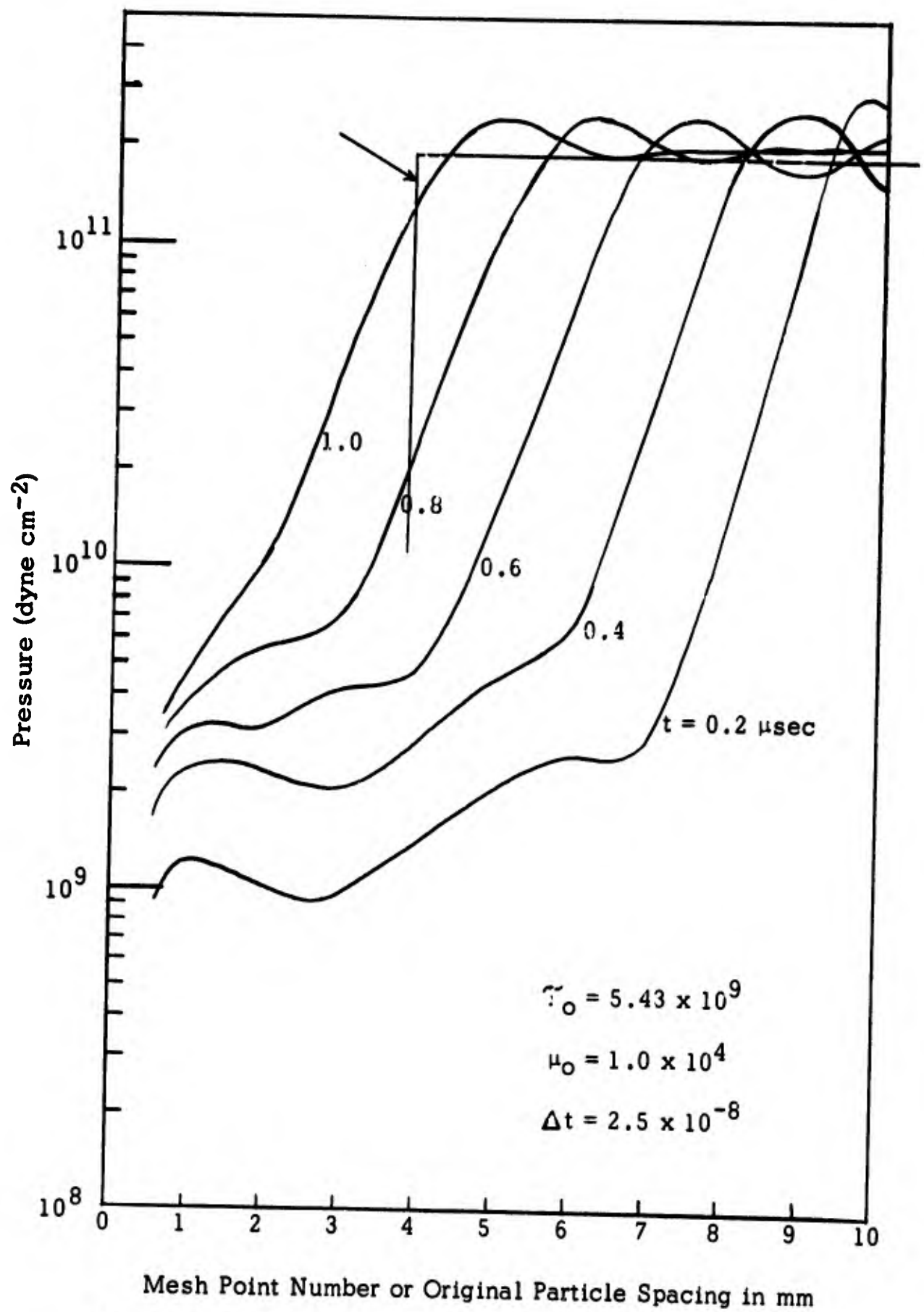


Figure 9. Pressure wave in one-dimensional impact in aluminum. Figures 8, 9 and 10 show the effects of varying viscosity. Corrector used twice in all cases. Curve marked "Theory" is from analytical calculations at $t = 1.0 \mu\text{sec}$.

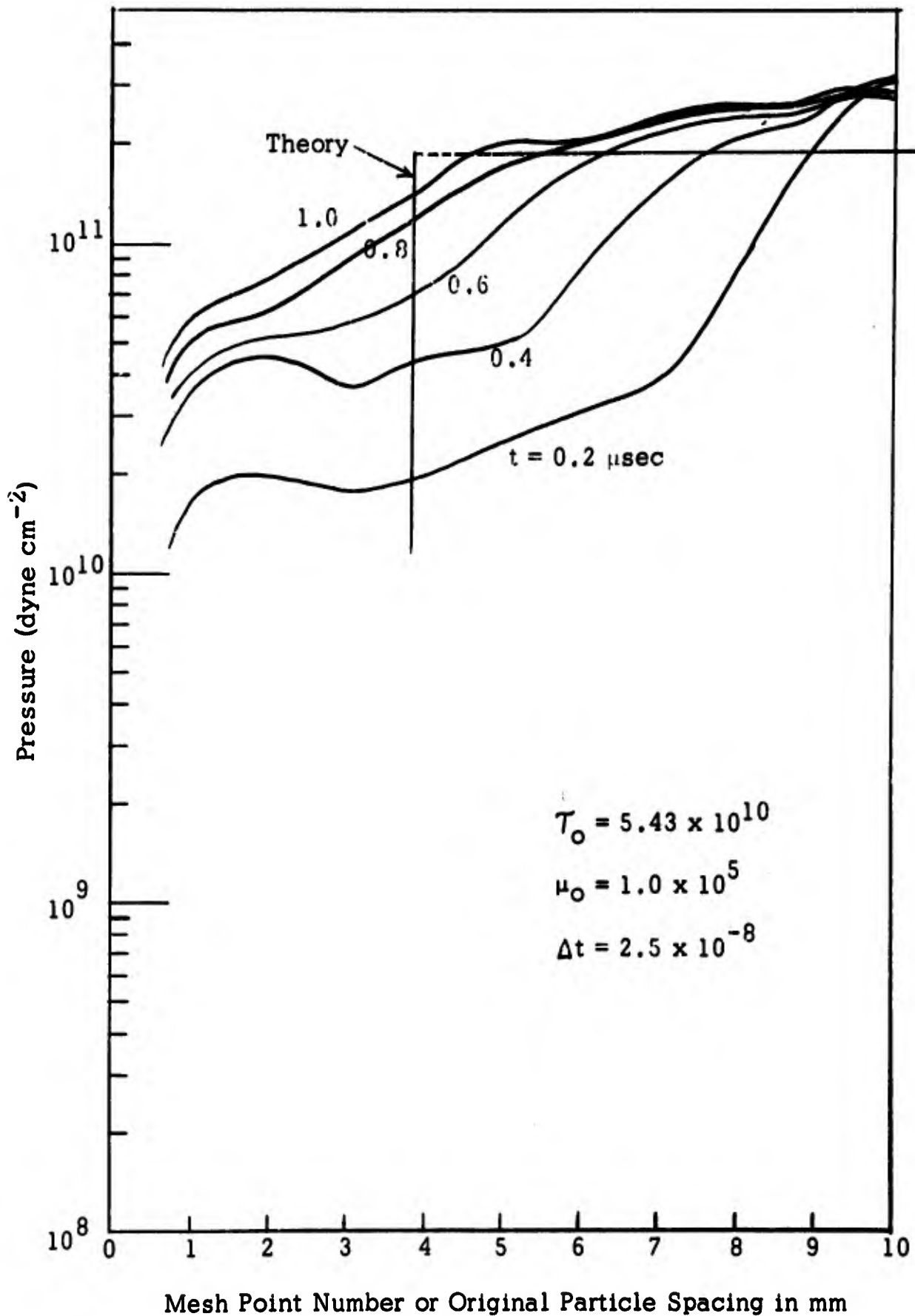


Figure 10. Pressure wave in one-dimensional impact in aluminum. Figures 8, 9 and 10 show the effects of varying viscosity. Corrector used twice in all cases. Curve marked "Theory" is from analytical calculations at $t = 1.0 \mu\text{sec}$.

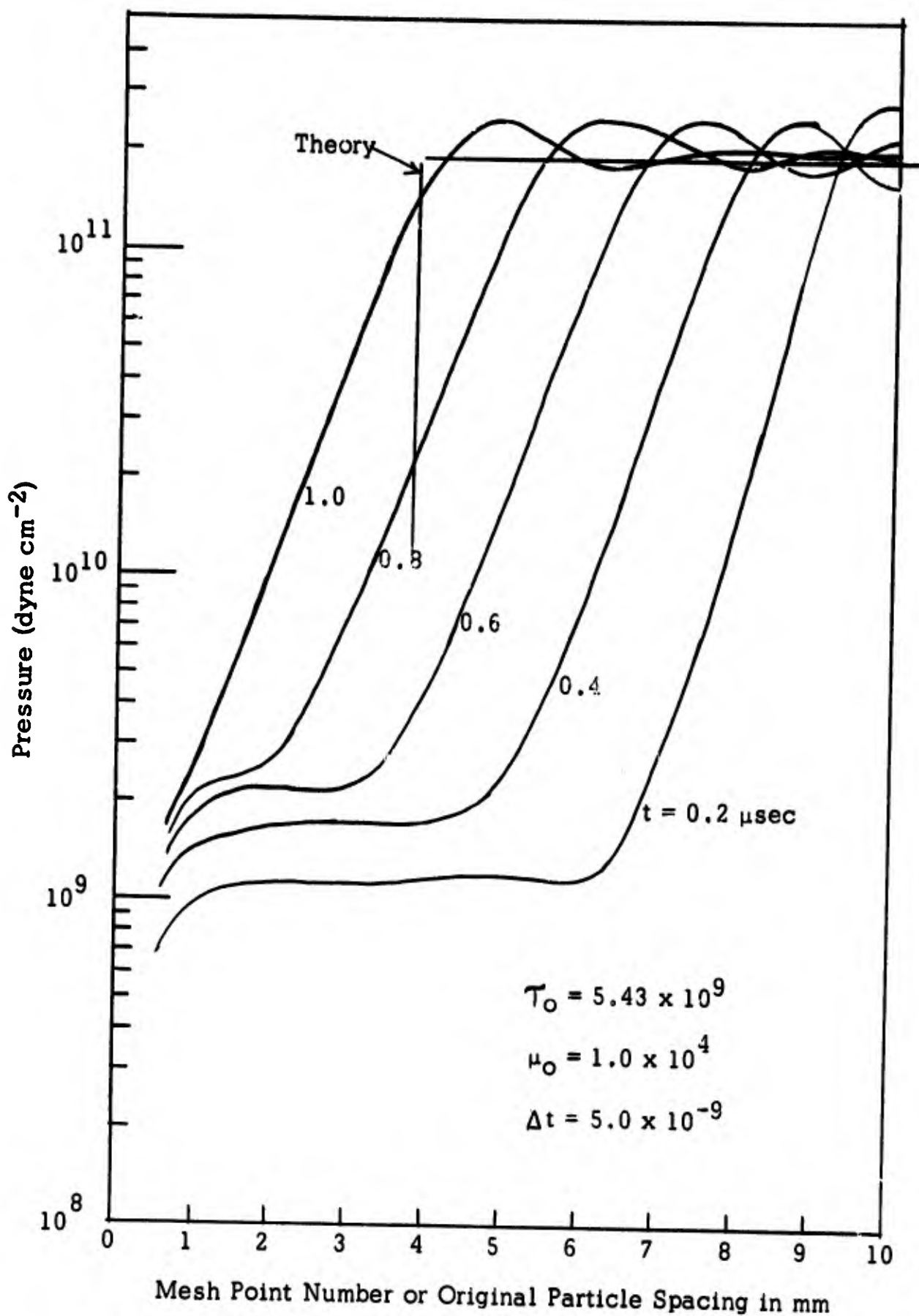


Figure 11. Pressure wave in one-dimensional impact in aluminum. Calculation made to show the effect of decreasing the time increment used. Compare with Figure 9. Corrector used twice.

3. EXPERIMENTAL WORK

3.1 Disc-Crushing Experiment

During this report period some experimental work was done to complete the work done on the disc-crushing experiment. This was aimed primarily at determining how much of the energy measured going into crushing of the disc was due to frictional loss with the anvil surfaces and how much was actually due to internal deformation of the disc. Tests were made by deforming a rod in tension in a testing machine, measuring the energy involved, and measuring the deformation on the same basis as used in the disc-crushing experiment. It was found that friction required a fair-sized correction to be made in the energy but not large enough to invalidate the results. If the correction were considerably in error, it would not change the general conclusions. It was found that with the copper discs at large deformations, about 25 per cent of the energy results from friction with the disc faces. This was also checked by shooting a steel ball into a plate and measuring the deformation there. As has been reported previously, all these measurements are in good agreement and are in agreement with earlier work done on rod-to-rod impact where the internal energy is measured by the measurement of velocity changes in an inelastic collision. In tension tests and in rod-to-rod impact, the deformation is measured by changes in thickness and diameter of circular-disc sections of the rods.

3.2 Dynamic Strength Measurements

The major experimental work of this report period has been the measurement of strength of materials under dynamic conditions. In doing the disc-crushing experiments, attempts were made to make measurements on plastics. This proved to be feasible with only a few materials under limited conditions. Measurements of deformation were hindered by plastic recovery, and shattering under impact. To obtain some measurement of the "strength" of materials under impact conditions, a rod-to-rod impact experiment was devised. In this experiment, a projectile rod is impacted against a stationary target rod and the acceleration of the rear face of the target rod is measured. From the force or momentum equation, it is seen that this measurement gives a gross measurement of an effective pressure gradient.

As the impact velocity is increased, it is of interest to see whether the acceleration (pressure gradient) reaches a maximum, indicating the maximum effective strength of the material. This value can be used in the

theoretical program or just as a means of rating different materials for use under impact conditions. Exploratory work to determine this maximum was carried out with glass, polypropylene, nylon, plexiglass and a compressed wood fiber called Benelex 70. The development of the experimental system and the results will be discussed in the following sections.

3.2.1 Experimental System for Dynamic Measurements

The system used to make the desired measurements was built up around devices which indicate the time-position history of the flat end of a rod from measurements of the total light intensity from an illuminated slit which is covered or uncovered by the moving rod. A schematic diagram of the system is shown in Figure 12. Not all possible measurements indicated were made on each shot. Rods were 1.000 inch length, 0.500 inch diameter.

The optical system was designed to permit the following measurements:

1. Velocity of the projectile at the time of impact with the target. This allows impact pressure to be determined.
2. Time of impact upon target. This gives wave-velocity data.
3. Time-position history of rear target face after impact. Differentiating this curve twice gives acceleration data and thus pressure gradient data.
4. Velocity of target after acceleration. This allows calibration of the acceleration curve.

Of the four measurements required, it was found that determining the time of projectile impact upon the target was the most difficult. One method tried was to pass a beam of light in front of the target rod and observe its intensity as the projectile impacted the target. It was expected that when the projectile closed the gap in front of the target, the time of impact could be determined as that moment when all the light was cut off. This method was useful at low velocities, but at high velocities it became difficult to determine just when the light was at zero. The oscilloscope trace was rounded rather than showing a sharp break. Later it was discovered that this was due to the generation of light at impact in the transparent plastics used. Also, the target rod sometimes appeared to move from air shock and vibration before impact.

A simple wire make-circuit was substituted for the first light slit and gives better results. The impact end of the target is painted with

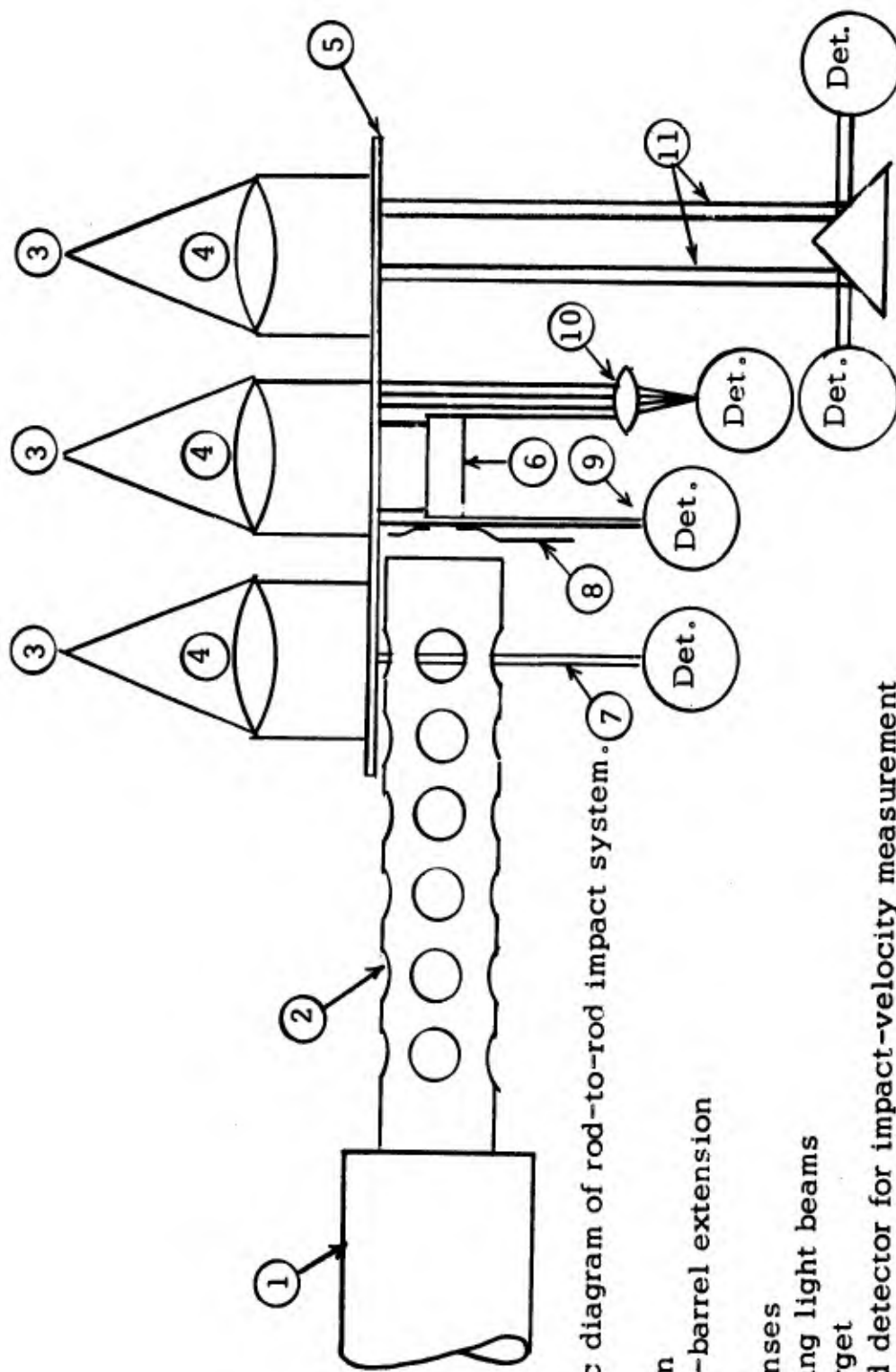


Figure 12. Schematic diagram of rod-to-rod impact system.

- 1. 50-cal. air gun
- 2. Perforated gun-barrel extension
- 3. Light sources
- 4. Collimating lenses
- 5. Slits for defining light beams
- 6. Cylindrical target
- 7. Light beam and detector for impact-velocity measurement
- 8. Make-wire circuit for impact-velocity measurement
- 9. Light beam and detector for impact-velocity measurement
- 10. Single or double light beam with collimator and detector for measuring target-rod acceleration and velocity
- 11. Double beam with prism and detector for measuring target-rod velocity

conducting silver paint and two small bare wires are suspended in front of the target. When the projectile pushes the wires into the silver paint, the circuit is closed. At first, a charged capacitor, discharged into a pulse-forming circuit, providing a pulse to the oscilloscope. This proved to be more reliable than the other methods tried, but still gave some trouble due to the high voltage across the break wires. Some premature discharging of the capacitor was experienced. This was improved by using a low voltage battery which shifted the oscilloscope trace when the make-wires were shorted.

The acceleration of the rear target face was measured using a light beam which intercepted the rear face. Figure 13 shows an oscilloscope trace produced as the target rod moves and cuts off the beam.

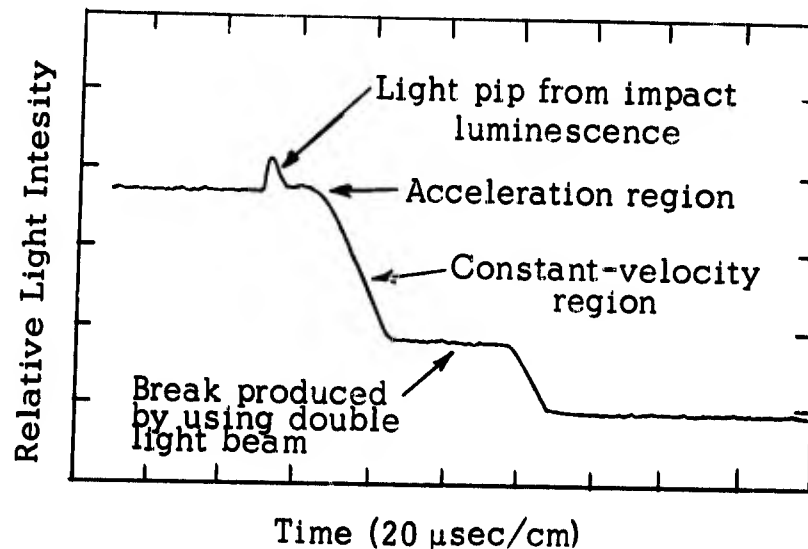


Figure 13. Oscilloscope trace from photomultiplier observing rear end of target rod. A double light beam of known spacing is used to give an internal velocity calibration so that an absolute velocity measurement is available for any slope on the trace. The light pip is ordinarily eliminated by painting rods.

The source of the pip of light on the oscilloscope traces which occurred at or about the time of impact was found by shooting a projectile into a target with all things normal except with no light present. The pip on the oscilloscope trace was still evident. Subsequent investigation revealed that a luminescence was taking place upon impact and increasing in intensity as the impact pressure increased. No further study was made to determine whether or not the intensity of the light was directly proportional to an increase in impact pressure or just where the upper and lower limits might be.

At first it was believed that this pip could be used to indicate the time of impact upon the target, but after a number of shots were made, it became evident that controlling the pip would be a problem and that it interfered with the acceleration curve in too many instances. The pip was eliminated by painting the target rod black.

Much difficulty was experienced at higher impact velocities in obtaining a target velocity. This was caused by the target rod breaking into small pieces before the velocity-measuring station was reached thus giving very erratic data. To overcome this problem, the slit at the rear of the target rod was modified to a double slit to give a step in the oscilloscope trace. Knowing the distance between the two light beams, the velocity of the target rod can be calculated, thereby obtaining a rod velocity before fragmentation can take place.

The linearity of the system was checked by shooting a projectile through the light beam at a constant velocity with no target in place. It was learned that some non-linearity was present in the photomultiplier tube and that this could be eliminated by collecting all light across the slit into a point and carefully selecting a spot on the photo-sensitive tube which gave the best response.

The linearity of the photomultiplier and associated electronics was checked by using a rotating disc. A slit was cut in the disc which would pass a beam of light into the photomultiplier once each revolution. By synchronizing the rotation of the disc with the sweep of an oscilloscope a photograph of the rise and fall was obtained. This was determined to be about $0.1 \mu\text{sec}$, which was well within the time requirements of the event being measured. The size and shape of the slit was also varied to show that these factors had little effect upon the shape and rise time of the light pulses.

A spark source with a known rise time of $0.5 \mu\text{sec}$ was used to check the response of the photomultiplier system. It was suspected that the target was moving before actual impact due to vibration caused by

shock waves or by air pressure ahead of the projectile. This was checked by shooting into a target firmly secured to the support platform. It was determined that some movement had been taking place and that a small amount of silicone grease between the target and its support platform would eliminate this without adding a significant amount of resistance to acceleration caused by projectile impact.

3.2.2 Data from Dynamic Measurements

Data from rod-impact experiments are shown in Figures 14 to 17. The results show considerable scatter due to material variability, experimental variations and the uncertainties in taking the second derivative of an experimental curve. However, general trends are clearly illustrated. The plastics tested reach a maximum and possibly even have a peak in the pressure gradient which they sustain. Benelex shows no peak in the range covered. Glass behaves very differently and no maximum "strength" is indicated.

These data will be extended to higher velocities by using a powder gun. Impact pressure will be increased by using massive hardened-steel projectiles. Some further exploratory work is planned to determine the effects of sizes of rods and to see how much of the observed effect is due to a one-dimensional crushing strength of the material or due to a flow or breakup of the material and a two-dimensional deformation.

Just how these strength measurements will fit into the theoretical program is not certain at this time. It is planned to begin to use them nearly exactly the same as the metal properties have been used; that is, the maximum acceleration observed, or maximum pressure gradient, will be related to the constant strength term in the Bingham model. It is likely that the viscous term depending on velocity gradient will be energy-sensitive or will depend on total deformation. It can possibly be determined from the way maximum pressure gradient changes with velocity of impact. We expect that the initial strength term will be predominant.

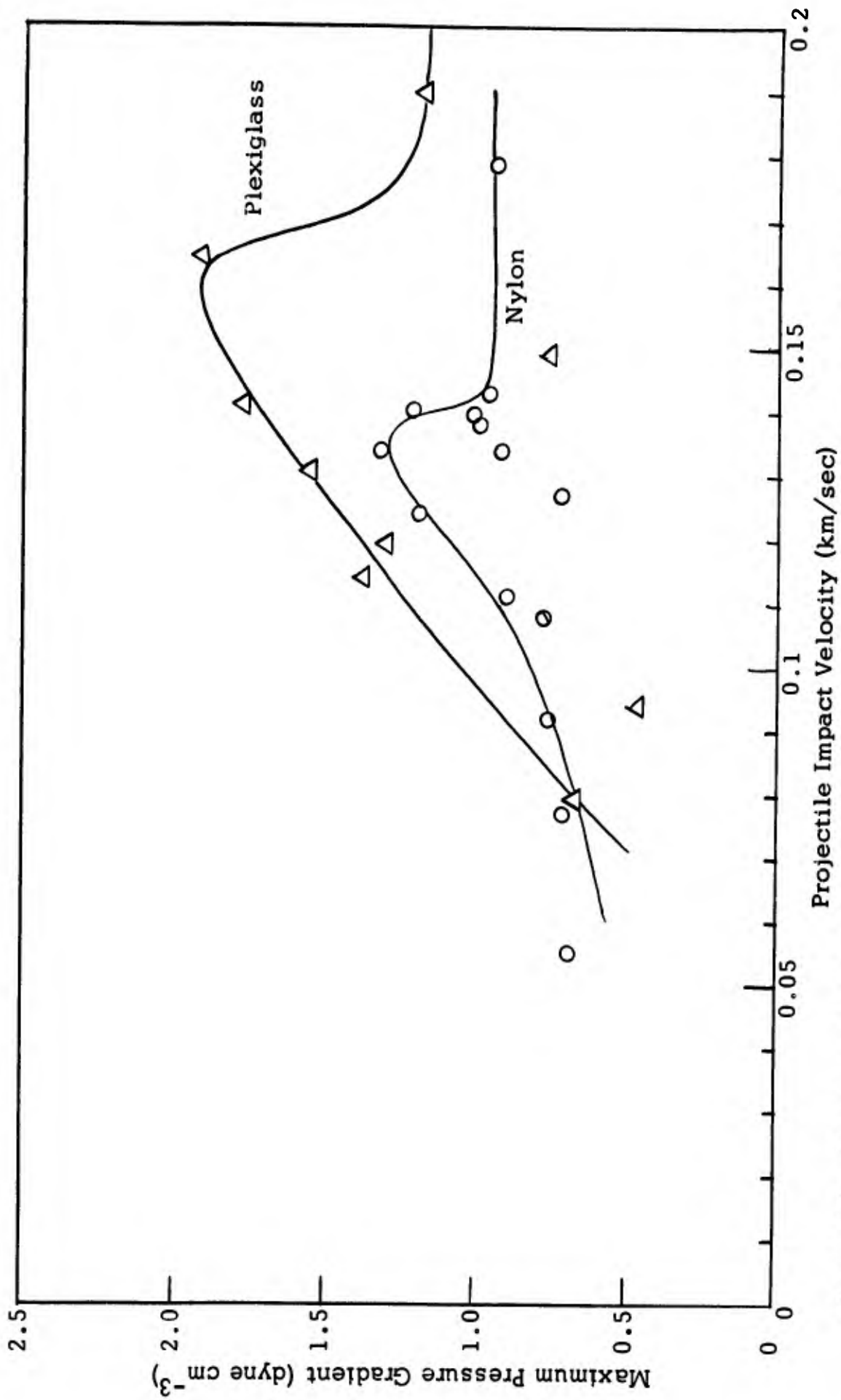


Figure 14. Maximum pressure gradient observed in rod-to-rod impact as a function of impact velocity. Pressure gradient given as $\rho dv/dx$ where ρ is material density and dv/dx is maximum measured acceleration of end of target rod.

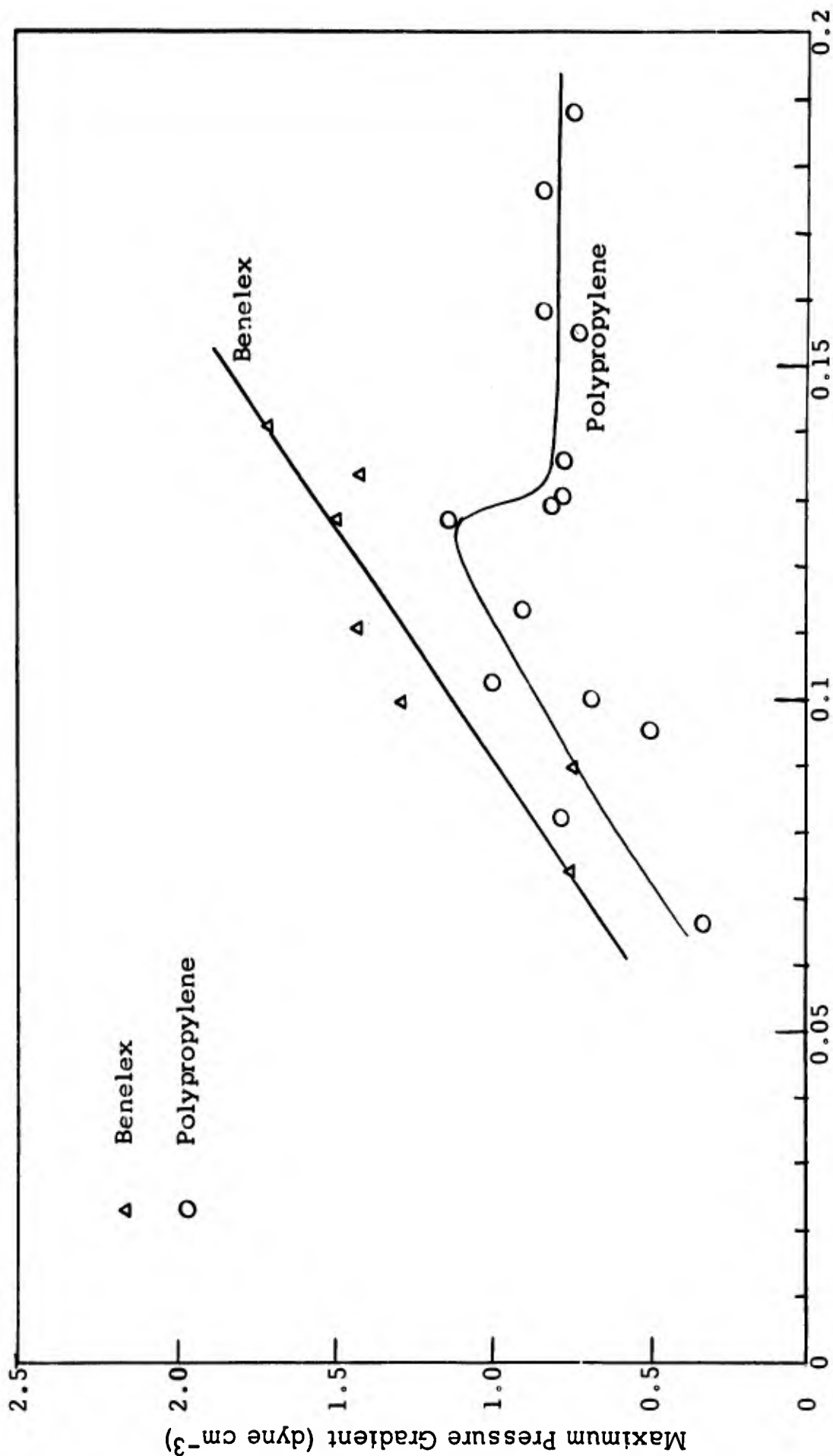


Figure 15. Maximum pressure gradient observed in rod-to-rod impact as a function of impact velocity. Pressure gradient given as $\rho \frac{dv}{dx}$ where ρ is material density and $\frac{dv}{dx}$ is maximum measured acceleration of end of target rod.

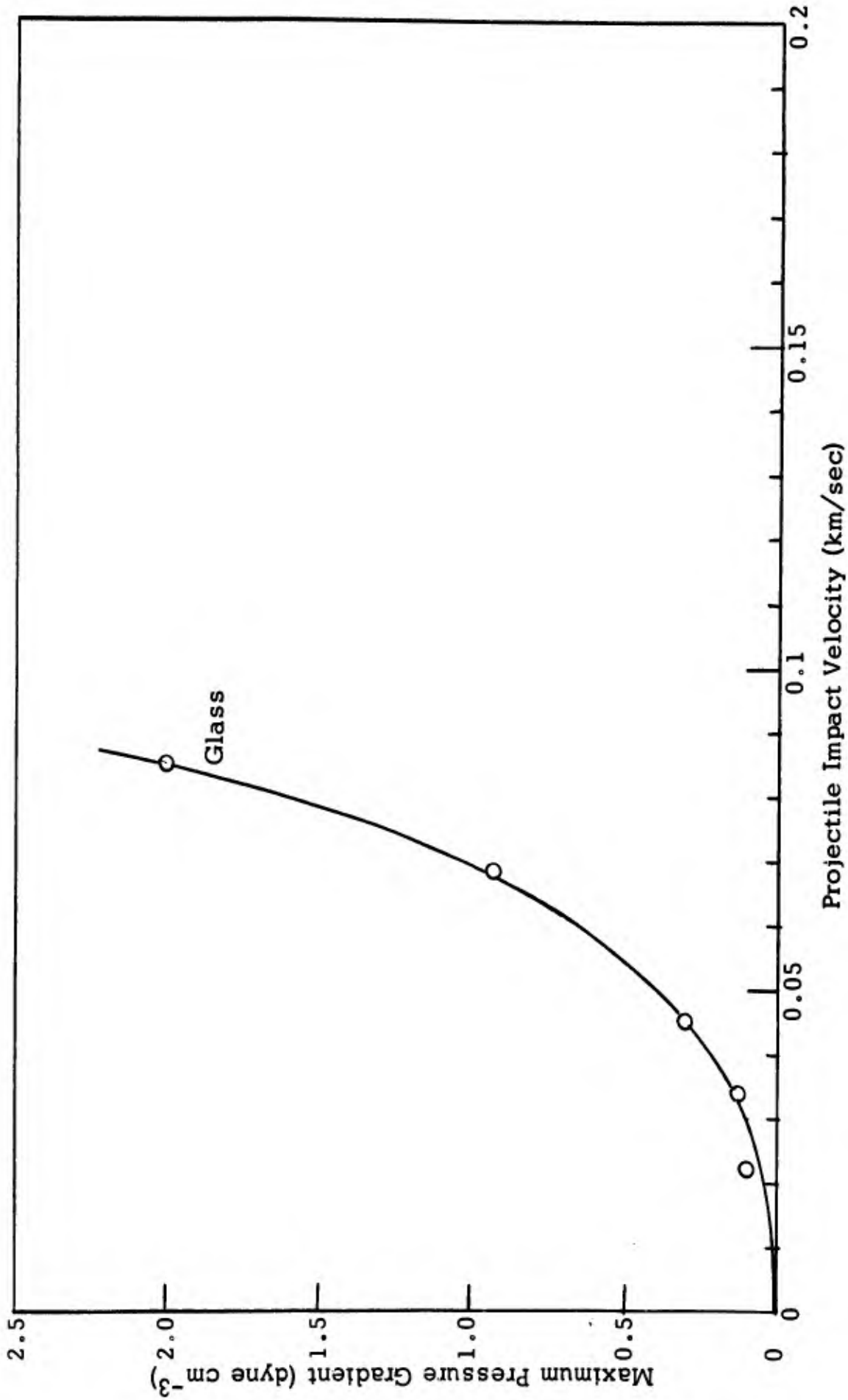
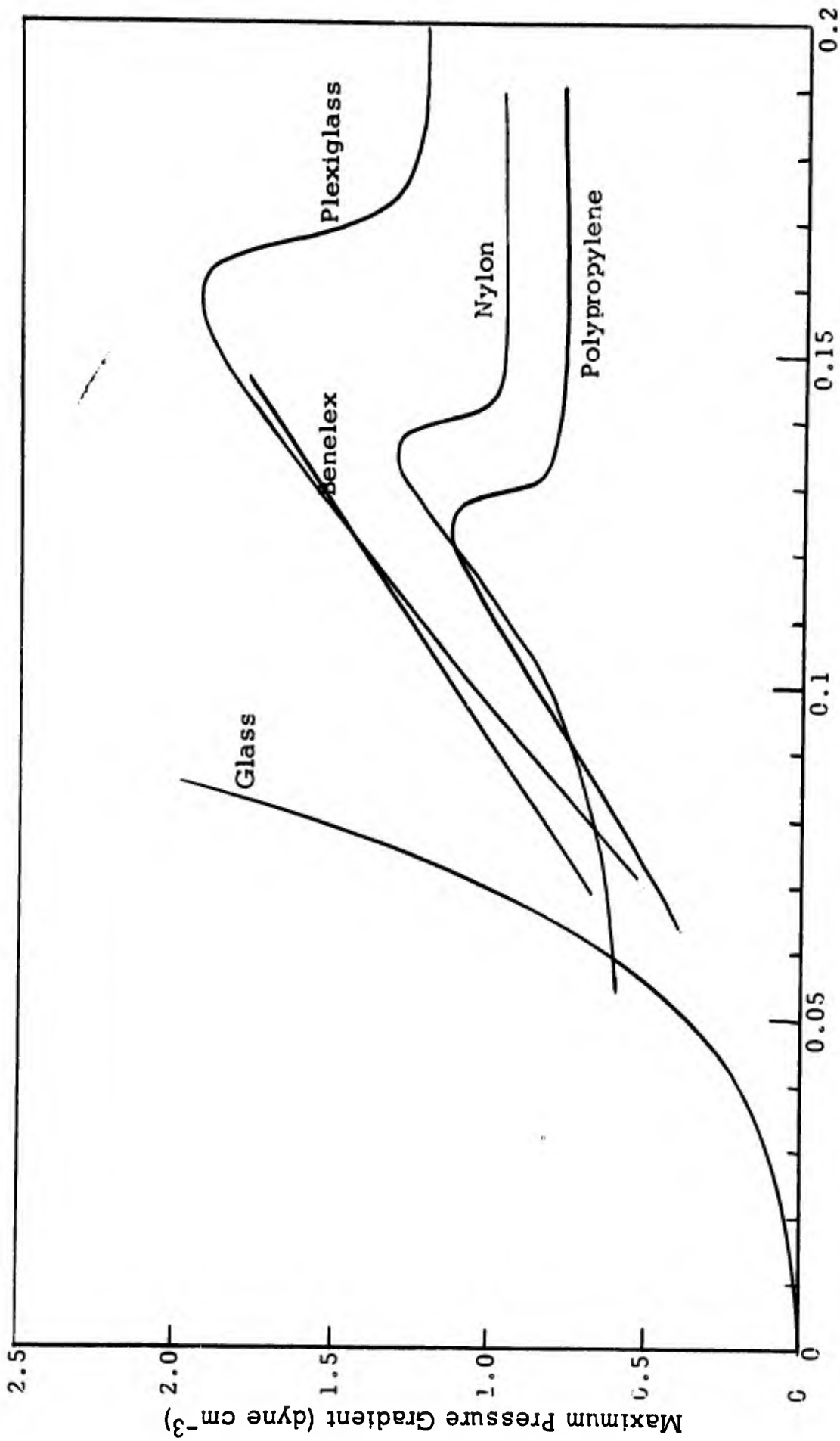


Figure 16. Maximum pressure gradient observed in rod-to-rod impact as a function of impact velocity. Pressure gradient given as $\rho \, dv/dx$ where ρ is material density and dv/dx is maximum measured acceleration of end of target rod.



Projectile Impact Velocity (km/sec)

Figure 17. Maximum pressure gradient observed in rod-to-rod impact as a function of impact velocity. Pressure gradient given as $\rho \frac{dv}{dx}$ where ρ is material density and $\frac{dv}{dx}$ is maximum measured acceleration of end of target rod. Data from Figures 14, 15 and 16 are compared.

4. CONCLUSIONS

The work of this report period justifies our earlier decision to base a computer program on a correct predictor/corrector scheme. The problems have not been solved, but the value of a proper predictor/corrector has been shown and its importance in controlling the wave front and in controlling the instabilities in the program have been indicated. The propagation of unwanted energy throughout the mesh remains a problem of the immediate future. It appears that some compromise will be necessary to obtain the best results from a predictor/corrector and the most freedom from unwanted error propagation. The use of proper strength and viscosity terms, even in one-dimensional impact, is shown to be very important. The values of strength and viscosity determined here are of significance in relation to the work of Riney, Bjork, Walsh and others studying high velocity impact. The experimental work has shown that under dynamic conditions, strength of material can be measured and indicates that useful data can be obtained from rod-to-rod impact. The use of these data in rating materials or in more complete theoretical work is yet to be investigated.

5. FUTURE WORK

The work of the next report period will consist of revisions of the mathematical model and the computer code to better describe one-dimensional impact and the development of a three-dimensional code for axisymmetric cases. The relationship of viscosity and strength to irreversible shock heating and to deposition of energy in impacted material will be investigated. Experimental work will consist of further exploratory work in brittle materials, particularly glass and ceramics, and further refinement of the measurement techniques. Different size samples will be used in order to obtain data to be used in the theoretical program and in general classifications of materials.